Anisotropic Repulsion Potentials for Cyanuric Chloride ($C_3N_3Cl_3$) and Their Application to Modeling the Crystal Structures of Azaaromatic Chlorides

John B. O. Mitchell[†] and Sarah L. Price*

Centre for Theoretical and Computational Chemistry, Department of Chemistry, University College London, 20 Gordon Street, London WC1H 0AJ, U.K.

Maurice Leslie

CCLRC Daresbury Laboratory, Warrington WA4 4AD, U.K.

David Buttar

AstraZeneca, Mereside, Alderley Park, Macclesfield, Cheshire SK10 4TG, U.K.

Ron J. Roberts

AstraZeneca, Silk Road Business Park, Charter Way, Macclesfield, Cheshire SK10 2NA, U.K.

Received: July 5, 2001; In Final Form: August 27, 2001

A series of nonempirical intermolecular potentials has been developed for the cyanuric chloride dimer, using the overlap model to determine the anisotropy of the repulsive wall around each atom. Calibration against intermolecular perturbation theory calculations enables the penetration and charge-transfer energy to be explicitly included with the exchange-repulsion to give a simple repulsion model in an anisotropic atom−atom form. These model repulsion potentials are used in conjunction with an atomic multipole electrostatic model and an atom−atom dispersion model to give nonempirical potential models, which are tested for their ability to reproduce the crystal structure of cyanuric chloride. The best nonempirical potential is successfully used to construct a simpler transferable model for closely related azaaromatic chlorides. The nonempirical potential reproduces the experimental space group of cyanuric chloride, unlike some empirically fitted repulsion−dispersion potentials. This first nonempirical repulsion potential to model the polar flattening of Cl atoms also reproduces the N···Cl and Cl···Cl interactions in other crystal structures.

1. Introduction

The assumption that organic molecules interact with each other as if they are composed of spherical atoms[1,2] is computationally convenient. Hence simulations of organic molecules in the solid or liquid state, or in complexes, have almost always used isotropic atom−atom model intermolecular potentials.[3] However, X-ray deformation density maps show that the charge distribution around an atom in a molecule often has a significant nonspherical component, such as lone pair and π electron density etc. Such nonspherical features give rise to atomic dipoles, quadrupoles, etc. in any complete representation of the molecular charge distribution,[3] such as provided by a distributed multipole analysis. The importance of the electrostatic forces arising from the nonspherical features in the charge distribution has been shown by the marked superiority of atomic multipole over atomic charge electrostatic models in predicting the structures of van der Waals complexes.[4] Distributed multipole electrostatic models also produce satisfactory models for the crystal structures of a wide range of polar organic molecules.[2,5]

The nonsphericity of the atoms within an organic molecule will also give rise to atom−atom anisotropy in the other terms in the intermolecular potential. The importance of this anisotropy in the repulsive short-range term has been often recognized[1] for accurate intermolecular potentials for small polyatomic molecules. It is required to represent ab initio potential energy surfaces for the dimers of N_2[6] and HF[7] and to reproduce the experimental data on HCl in van der Waals complexes.[8] For Cl_2, it plays a particularly significant role in accounting for the herringbone layer *Cmca* crystal structure.[9] Analysis of the effective van der Waals contact distances of atoms bonded to carbon (X−C) in the organic crystal structures within the Cambridge Structural Database has shown[10] that atoms such as Cl, Br, I, S, and Se in organic crystals appear to have an anisotropic van der Waals "radius". The polar flattening of organic chlorine atoms, where significantly closer approach of the atoms is possible for head-on rather than sideways contacts, has led to considerable speculation as to whether this represents a specific orientation dependent attractive force,[11] or anisotropy in the repulsion.[12] However, intermolecular perturbation theory calculations on the CH_3Cl dimer demonstrate[12] that there is marked anisotropy in the exchange-repulsion energy, which, combined with the anisotropic electrostatic interaction, accounts for the anisotropy in the effective van der Waals radius of organic chlorine. Crystal database analyses[13] of contacts between halogens and nitrogen or oxygen show a preference for Cl, Br, and I to form short contacts with O or N along the C−X bond axes, with interatomic separations less than the sum of traditional van der Waals radii. Calculations on model systems for Cl···O

* Author for correspondence. Fax: 44-20-7679-7463; E-mail: s.l.price@ucl.ac.uk.

[†] Current Address: Department of Chemistry, University of Cambridge, Lensfield Road, Cambridge CB2 1EW, U.K.

10.1021/jp0125350 CCC: $20.00
Published on Web 10/02/2001

SCHEME 1: Azaaromatics Cyanuric Chloride (VUGSIZ), 2,4,6,8-Tetrachloropyrimido[5,4-*d*]pyrimidine (PIJBIT) and 2,4,6,7-Tetrachloropteridine (PIJBOZ)[a]

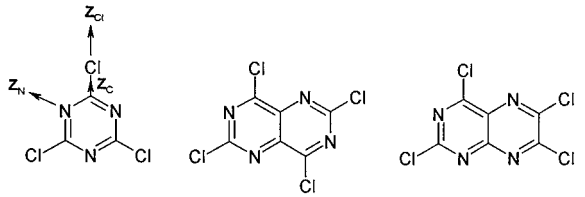

VUGSIZ PIJBIT PIJBOZ

[a] The definition of the atomic local axes for Cl, C, and N atoms is shown for example on atoms of VUGSIZ.

and Cl···N contacts show that this directionality is primarily the result of the anisotropic distribution of electron density around the halogen nucleus, leading to a significant angular dependence in the exchange-repulsion.[13] This allows closer approach to the Cl in the head-on direction when favored by an attractive electrostatic interaction.

To go from acknowledging that the atom−atom repulsion involving chlorine atoms is orientation dependent, to actually implementing an anisotropic atom−atom model potential capable of reproducing its effect on close contact distances, requires a method of parametrizing this anisotropy. Although it is possible to empirically fit an anisotropic repulsion model for the crystal structure of Cl_2,[14] this is not practical for organic molecules. This is because the number of atomic types in organic molecules requires a large number of isotropic parameters to be derived empirically. Indeed, when isotropic empirical Cl repulsion−dispersion parameters were obtained[15] by fitting to crystal structures and heats of sublimation of perchlorinated hydrocarbons, combining rules had to be assumed to reduce the number of parameters. These isotropic potentials are adequate within the usual criterion for lattice energy minima calculated from empirical potentials to reproduce room-temperature crystal structures. Hence the functional form of the anisotropy, and the parameters, have to be obtained by a nonempirical method.

We have been developing the use of the overlap model to provide nonempirical parameters for atom−atom potentials to represent the short-range repulsive potentials for organic molecules.[16−19] This method uses an assumed proportionality between the exchange-repulsion, and penetration (and optionally, and less accurately, charge-transfer) energy and the overlap of the ab initio molecular charge densities at the specific relative orientation of the two molecules. This overlap can be computed far more cheaply than intermolecular interaction energies (for the same level of ab initio theory), and vitally, can be broken down into atom−atom contributions through a division of the molecular charge distribution into atomic contributions.[20,21] Thus, the anisotropy of, for example, the Cl···N repulsion can be obtained by fitting to a large data set of Cl···N overlaps, representing the range of relative separations and orientations of the two atoms that could be sampled by any simulation of the properties of the pair of molecules. This paper derives the first anisotropic atom−atom repulsion potentials for organic molecules using this approach.

The first application of this method is to cyanuric chloride ($C_3N_3Cl_3$, Scheme 1), as it has been proposed[22] that the crystal structure of cyanuric chloride is evidence for the importance of anisotropy in the N···Cl interaction influencing a crystal structure. The crystal structure of cyanuric chloride consists of layers, rather than the "herringbone" structure usually found for similar compounds with idealized D_{3h} symmetry.[23] Within the layers, the structure is held together by C−Cl···N interactions. These have a geometrical resemblance to hydrogen bonds, with the N···Cl−C angle being 180° for Cl1 and 173° for Cl2 and Cl3. The Cl···N intermolecular contacts of 3.10 and 3.11 Å, respectively,[22] are considerably shorter than the sum of the van der Waals radii. The deviation of contacts from linearity produces a "fish-scale" effect, with the molecular planes tilted by 3° to the layer plane. This fish-scale effect was not reproduced[22] in crystal structure modeling using the empirical force fields then implemented in the Cerius software.[24] This led Maginn et al. to conclude that "current sets of isotropic interatomic potentials are insufficient to successfully predict the observed crystal structure of cyanuric chloride" and to speculate whether anisotropic interatomic potentials for chlorine would successfully predict the observed structure.

Cyanuric chloride is an industrially important molecule, used mainly to provide the 1,3,5-triazine functionality in the production of reactive dyes, optical brighteners, herbicides, and pharmaceuticals.[25] Therefore, it is essential to obtain a reliable intermolecular potential for investigation of its possible polymorphism by lattice energy minimization methods of crystal structure prediction.[26] It also provides a model for the C−Cl···N interaction, which, with its preference for linearity, has been exploited to some degree for the design of crystalline organic solids.[27] The energy of this "donor−acceptor" interaction is considered to be significantly weaker than a hydrogen bond, with an MP2 supermolecule calculation[27] on a model system giving a value of 5.1 kJ/mol. Nevertheless, its role in a variety of crystal structures is sufficiently important[27] that a transferable model potential is required.

The crystal structure of cyanuric chloride also involves Cl···Cl interactions and the stacking of aromatic π systems, and hence the balance between these interactions. The generality of the derived nonempirical model potential, including the anisotropic terms, can be tested for its transferability to two closely related molecules (Scheme 1), whose crystal structures[27] are also determined by C−Cl···N(aromatic) contacts. 2,4,6,8-Tetrachloropyrimido[5,4-*d*]pyrimidine (PIJBIT, Scheme 1) adopts a layered crystal structure similar to that of cyanuric chloride, with each molecule having eight Cl···N contacts. In contrast, 2,4,6,7-tetrachloropteridine (PIJBOZ, Scheme 1) has a completely different 3D herringbone crystal structure, where only half the nitrogen and chlorine atoms are involved in Cl···N contacts

Thus this paper first develops a nonempirical anisotropic atom−atom potential for cyanuric chloride, with the novel development of an anisotropic atom−atom repulsion model. We first contrast the fitting of isotropic and anisotropic models to the atom−atom overlaps. Then intermolecular perturbation theory (IMPT)[3,28,29] calculations for the exchange-repulsion, penetration, and charge-transfer energies for a range of dimer geometries are employed to fix the proportionality parameters for the repulsion models and to simultaneously validate the derived repulsion model.

The short range repulsion potentials for cyanuric chloride are then combined with an accurate distributed multipole electrostatic model (also derived from the wave function of the isolated molecule) and an atom−atom dispersion model to give totally nonempirical intermolecular pair potentials. These are tested for their ability to reproduce the crystal structure of cyanuric chloride by lattice minimization. The best cyanuric chloride potential is adapted to provide a transferable model potential for the larger molecules in Scheme 1, which are too large for the derivation of a molecule-specific potential. The combined

results are used to assess the method of potential derivation and also to discuss the modeling of the C−Cl···N interaction and the origin of the "fish-scale" effect.

2. Method of Derivation of the Intermolecular Potential Model

We use an atom−atom form for the intermolecular energy between cyanuric chloride molecules A and B,

$$U = \sum_{i\in A,k\in B} A_{\iota\kappa} \exp(-B_{\iota\kappa}(R_{ik} - \rho_{\iota\kappa}(\Omega_{ik}))) - C_{\iota\kappa}/R_{ik}^{\,6} + U_{\mathrm{elec}}(\mathrm{DMA},\Omega_{ik},R_{ik}^{\,-n},n\leq 5) \quad (1)$$

where atom i in molecule A and k in molecule B are of atom types ι and κ, respectively, and are separated by a distance R_{ik} with a relative orientation Ω_{ik} defined by local axes along the covalent bonds.

The nonempirical dispersion coefficients $C_{\iota\kappa}$ are taken from C_6 atom−atom parameters for C···C, N···N, and C···N derived from density functional calculations, averaging over several compounds.[30] The $C_{\iota\kappa}$ for Cl···Cl are estimated from experimental atomic polarizabilities,[31] and the C···Cl and N···Cl dispersion coefficients were derived by a geometric mean combining rule. The electrostatic model includes all terms in the atom−atom multipole series up to R_{ik}^{-5} arising from the atomic multipole moments (charge, dipole, quadrupole, octupole, and hexadecapole) obtained by a distributed multipole analysis[32] of the ab initio wave function of the isolated molecule. The model potential thus only differs in functional form from the empirical atom−atom plus distributed multipole model that we have previously used in modeling organic crystal structures,[5] in that the term $\rho_{\iota\kappa}(\Omega_{ik})$ introduces anisotropy into the atom−atom repulsion.

The functional form used for the atom−atom repulsion is

$$\rho_{\iota\kappa}(\Omega_{ik}) = \rho_1^{\,\iota}(\mathbf{z}_i\cdot\mathbf{R}_{ik}) + \rho_1^{\,\kappa}(-\mathbf{z}_k\cdot\mathbf{R}_{ik}) + \rho_2^{\,\iota}(3[\mathbf{z}_i\cdot\mathbf{R}_{ik}]^2 - 1)/2 + \rho_2^{\,\kappa}(3[\mathbf{z}_k\cdot\mathbf{R}_{ik}]^2 - 1)/2 \quad (2)$$

where $\mathbf{z}_i$ is the unit local axis vector of atom i and $\mathbf{R}_{ik}$ is the unit intermolecular atom−atom vector from atom i to atom k. In the case of cyanuric chloride, the local axis vectors for chlorine $\mathbf{z}_{Cl}$ and carbon $\mathbf{z}_C$ were defined along the bond from C to Cl (Scheme 1), and the nitrogen local axis $\mathbf{z}_N$ is defined to bisect the two covalent ring bonds, approximately in the direction of the ring center to nitrogen vector.

This functional form for the anisotropy has been derived from the general formulation of the repulsion energy[3]

$$E_{\mathrm{rep}} = \sum_{i\in A,k\in B} u \exp(-\alpha_{\iota\kappa}(\Omega_{ik})[R_{ik} - \rho_{\iota\kappa}(\Omega_{ik})]) \quad (3)$$

where

$$\rho(\Omega) = \sum \rho_{l_1l_2j}^{k_1k_2} \bar{S}_{l_1l_2j}^{k_1k_2}(\Omega)$$

and $\alpha(\Omega)$ are expanded in the set of general orientation dependent functions,[3] with the integer indices l_1, k_1, and l_2, k_2, denoting the rotational transformation characteristics with respect to the orientation of the atomic molecular fragment 1 and 2, and j with respect to the intersite vector. This form of expansion has been used for intermolecular forces,[3,33] including previous studies of anisotropic repulsion models.[19,34] The above definition (eq 3) has the property that the repulsion has the specific value of u energy units when $R_{ik} = \rho_{\iota\kappa}(\Omega_{ik})$. This form is equivalent to the repulsion term in (1), with $A = u \exp(\alpha\rho_{000}^{00})$.

In deriving the repulsion model for cyanuric chloride, we make the common simplification that the steepness of the repulsive wall, α, is independent of orientation. The anisotropy of the repulsion is now determined by $\rho(\Omega)$. We make the further assumption that each atom has a fixed anisotropic shape for the contours of the repulsive wall, so that the same anisotropic parameters for Cl are used to describe its interactions with C, N, or another Cl. Thus if the Cl is atom 1, then only $\bar{S}$ functions with $l_2 = k_2 = 0$ appear in the expansion of $\rho(\Omega)$. A more specific approximation made for cyanuric chloride, and monitored in the development of the potential, is that only the leading terms are required in which the C−Cl bond and the nitrogen lone pair have cylindrical symmetry. This cylindrical symmetry assumption means that only the local atomic **z** axes (Scheme 1) need to be defined, and only terms with $k = 0$ appear in the expansion. (Hence, from this point the k_1 and k_2 indices of zero will be omitted for clarity.) Thus using the first two terms in the expansion allows both a dipolar, ρ_1, and a quadrupolar, ρ_2, distortion of the atomic shape from spherical. When such a model for the anisotropic repulsion between atoms in homonuclear diatomics was considered,[35] modest nonspherical distortions produced significant changes in the relative lattice energies of the optimum crystal structures in different space groups.

Thus the model repulsive potential in (1) is formally equivalent to

$$E_{\mathrm{rep}} = \sum_{i\in A,k\in B} u \exp(-\alpha_{\iota\kappa}[R_{ik} - (\rho_0^{\,\iota\kappa} + \rho_{101}^{\,\iota}\bar{S}_{101} + \rho_{011}^{\,\kappa}\bar{S}_{011} + \rho_{202}^{\,\iota}\bar{S}_{202} + \rho_{022}^{\,\kappa}\bar{S}_{022})]) \quad (4)$$

with the implicit transferability that the parameters ρ_1Cl ($=\rho_{101}^{Cl} = \rho_{011}^{Cl}$), ρ_1N, ρ_1^C, ρ_2^{Cl}, ρ_2^N and ρ_2^C are constant across all relevant atom pairs.

2.1. Derivation of Repulsive Potentials from Overlap Calculations. The parametrization of the anisotropic repulsive potential is based on the assumption that the total repulsive energy is approximately proportional to the overlap, S_ρ, of the charge densities of the two monomers at all relative orientations, where

$$S_\rho = \int \rho_A(r)\,\rho_B(r)\,\mathrm{d}r \quad (5)$$

The accuracy of this assumption can be increased[16,34] by the introduction of a power law,

$$E_{\mathrm{rep}} = K[S_\rho]^y \quad (6)$$

with the power y being slightly less than 1.

The overlap is subdivided into atom−atom contributions, which are then fitted to an analytical model, with an accuracy that obviously depends on the assumed functional form, and can be assessed. The two parameters K and y are then derived. In this case, we use IMPT calculations of the exchange-repulsion, penetration, and charge transfer at a range of points on the potential energy surface both to determine the constants K and y and to validate the model against ab initio data, prior to testing against the experimental crystal structures.

2.1.1. Generation and Fitting of the Atom−Atom Overlap Model. The calculations of the overlap and of the distributed multipoles[32] were carried out using a D_{3h} molecular structure, which was obtained by 3-21G SCF geometry optimization (and is almost identical to the 6-311+G MP2 optimized structure of Pai et al.[36]). A 6-31G* MP2 wave function of this structure was calculated using CADPAC.[37] An atomic point multipole

TABLE 1: Parameters (in Atomic Units) for the Isotropic and Anisotropic Atom−Atom Models for the Intermolecular Overlap

	N···N	N···C	N···Cl	C···C	C···Cl	Cl···Cl
a_{ik}	2.297	2.233	2.163	2.317	2.537	2.103
${\chi_0}^{\iota\kappa}$ (iso)	2.177	1.725	2.290	1.642	2.651	2.710
${\chi_0}^{\iota\kappa}$ (aniso)	2.206	1.750	2.358	1.654	2.607	2.625
${\rho_1}^{\iota} = \rho_{101}$	−0.041725	−0.041725	−0.041725	−0.015962	−0.015962	0.050565
${\rho_1}^{\kappa} = \rho_{011}$	−0.041725	−0.015962	0.050565	−0.015962	0.050565	0.050565
${\rho_2}^{\iota} = \rho_{202}$	0.009218	0.009218	0.009218	0.018484	0.018484	−0.191144
${\rho_2}^{\kappa} = \rho_{022}$	0.009218	0.018484	−0.191144	0.018484	−0.191144	−0.191144

representation was obtained by a distributed multipole analysis (DMA) of this charge density, for use in modeling the electrostatic interactions. A Gaussian multipole representation,[38] which maintains the spatial extent of the charge density, was obtained by a GMUL[20,38] analysis, for use in calculating the charge overlaps. These two analyses subdivide the charge density into atomic contributions.

To sample the overlap as a function of the relative orientation, we generated 300 random geometries in which the two cyanuric chloride monomers are in approximate van der Waals contact (as defined by the radii C 1.7, N 1.5, and Cl 1.8 Å). At each of these dimer geometries, we used GMUL[21] to calculate the total charge overlap S_ρ (hereafter, "overlap") and its component atom−atom overlaps ${S_\rho}^{ik}$. The corresponding set of atom−atom distances, R_{ik}, and orientations, $\mathbf{z}_i\cdot\mathbf{R}_{ik}$ and $\mathbf{z}_k\cdot\mathbf{R}_{ik}$, were also calculated for each geometry. As the C···C interaction was rarely sampled in the randomly generated structures, nine extra stacked geometries were generated and used for parametrizing the C···C overlap.

For each atom pair, the atom−atom overlap was fitted to the appropriate functional form. This form has an isotropic version

$$ {S_{\mathrm{iso}}}^{ik} = s\exp(-\alpha_{\iota\kappa}[R_{ik} - {\chi_0}^{\iota\kappa}]) \tag{7} $$

and an anisotropic version

$$ \begin{aligned} {S_{\mathrm{aniso}}}^{ik} = s\exp(-\alpha_{\iota\kappa}[R_{ik} - ({\chi_0}^{\iota\kappa} + {\rho_1}^{\iota}(\mathbf{z}_i\cdot\mathbf{R}_{ik}) + \\ {\rho_1}^{\kappa}(-\mathbf{z}_k\cdot\mathbf{R}_{ik}) + {\rho_2}^{\iota}(3[\mathbf{z}_i\cdot\mathbf{R}_{ik}]^2 - 1)/2 + \\ \rho_2\kappa(3[\mathbf{z}_k\cdot\mathbf{R}_{ik}]^2 - 1)/2)]) \end{aligned} \tag{8} $$

The fixed parameter s is one unit of overlap, 1 atomic unit in this work. The decay constants $\alpha_{\iota\kappa}$ were first fitted to the separation dependence of the isotropic coefficient in GMUL's partial wave expansion of the atom−atom overlap.[16] The other parameters in eq 8 were then fitted to the GMUL atom−atom overlaps by first fitting ${\chi_0}^{\mathrm{ClCl}}$, ${\rho_1}^{\mathrm{Cl}}$, and ${\rho_2}^{\mathrm{Cl}}$ to the Cl···Cl overlaps, and ${\chi_0}^{\mathrm{NN}}$, ${\rho_1}^{\mathrm{N}}$, and ${\rho_2}^{\mathrm{N}}$ to the N···N overlaps. ${\chi_0}^{\mathrm{CCl}}$, ${\rho_1}^{\mathrm{C}}$, and ${\rho_2}^{\mathrm{C}}$ were fitted to the C···Cl overlaps, using the previously determined values for ${\rho_1}^{\mathrm{Cl}}$ and ${\rho_2}^{\mathrm{Cl}}$. The remaining χ_0 values only were fitted to the N···Cl, C···C, and C···N overlaps, using the previous values for the anisotropy coefficients. A fully isotropic model for the overlap (eq 7) was also determined by fitting χ_0 only to each set of overlaps.

For each atom−atom pair, only those contacts giving rise to GMUL atom−atom overlaps between 0.00005 and 0.005 atomic units were considered for the fitting. This corresponds to atom−atom exchange-repulsion energies between approximately 1 and 100 kJ/mol. This is a very generous coverage of the repulsive wall, as the higher energy regions are only likely to be sampled for orientations where the attractive forces are very strong at high temperatures. The parameters for fitting the overlaps with the isotropic and fully anisotropic model are given in Table 1. The trends in the isotropic parameters make chemical sense, with the overlaps involving chlorine atoms being consistent with its being the largest atom.

TABLE 2: Measures of the Importance of the Anisotropy in the Atom−Atom Intermolecular Overlaps[a]

atom pair type		correlation coeff	$\Delta S_{\mathrm{iso}}/\Delta S_{\mathrm{aniso}}$	derived	transferred
N	N	0.6660	1.80	N	
N	C	0.0888	1.01		N, C
N	Cl	0.9646	29.94		N, Cl
C	C	−0.1630	0.97		C
C	Cl	0.5485	1.43	C	Cl
Cl	Cl	0.9764	21.48	Cl	
total overlap		0.9726	10.44		

[a] The correlation coefficients between $\ln[S_\rho/S_{\mathrm{iso}}]$ and $\ln[S_{\mathrm{aniso}}/S_{\mathrm{iso}}]$ and the sum of squared errors ratio $\Delta S_{\mathrm{iso}}/\Delta S_{\mathrm{aniso}} = \Sigma(S_{\mathrm{iso}} - S_\rho)^2/\Sigma(S_{\mathrm{aniso}} - S_\rho)^2$ for the six atom type pairs and the total overlap. Data for the atom pairs are based on all generated geometries in which the relevant atom−atom overlap was between 0.00005 and 0.005 atomic units; data for total overlaps are based on the 20 geometries used for IMPT calculations. The last two columns show which anisotropic coefficients were derived by fitting to that set of atom−atom overlaps and which were transferred from fits to other types of overlaps.

The importance of including anisotropy in fitting the overlaps for each atom pair was measured by plotting $\ln[{S_\rho}^{ik}/{S_{\mathrm{iso}}}^{ik}]$ against $\ln[{S_{\mathrm{aniso}}}^{ik}/{S_{\mathrm{iso}}}^{ik}]$, where ${S_\rho}^{ik}$ (eq 5 partitioned into atomic contributions), ${S_{\mathrm{iso}}}^{ik}$ (eq 7), and ${S_{\mathrm{aniso}}}^{ik}$ (eq 8), are the accurately calculated, isotropically modeled, and anisotropically modeled atom−atom overlaps at each geometry, respectively. A high correlation coefficient between $\ln[S_\rho/S_{\mathrm{iso}}]$ and $\ln[S_{\mathrm{aniso}}/S_{\mathrm{iso}}]$ means that most of the deviation of S_ρ from a simple isotropic atom−atom exponential form is due to atom−atom anisotropy. A second measure of the importance of anisotropy is given by the ratio of the sum of squared errors in isotropic and anisotropic fits of the overlaps,

$$ \Delta {S_{\mathrm{iso}}}^{ik}/\Delta {S_{\mathrm{aniso}}}^{ik} = \Sigma({S_{\mathrm{aniso}}}^{ik} - {S_\rho}^{ik})^2/\Sigma({S_{\mathrm{iso}}}^{ik} - {S_\rho}^{ik})^2 \tag{9} $$

for each atom pair. The values of both measures for the six pairs of atom types, and the total overlap, are given in Table 2. The data show that incorporating anisotropy greatly improves the description of the overlap for Cl···Cl and N···Cl pairs, makes a small improvement for C···Cl and N···N, but has no effect for N···C and C···C. Thus, the anisotropy in the overlap associated with chlorine atoms is by far the most significant.

This is consistent with the largest anisotropic coefficients being associated with the chlorine atom (Table 1). By far the largest term is the negative ${\rho_2}^{\mathrm{Cl}}$, which produces a "quadrupolar" polar flattening, with reduced repulsion along the cylindrical axis of the C−Cl bond and an increased equatorial repulsion. This corresponds to the polar flattening of the effective van der Waals radius of Cl atoms in organic crystal structures.[10] This model of the shape is refined by a much smaller positive ${\rho_1}^{\mathrm{Cl}}$ coefficient. This term corresponds to a "dipolar" kind of polar flattening, with increased repulsion along the outward (or "intermolecular") direction of the cylindrical axis, decreased repulsion along the directly opposite and essentially unsampled inward direction (along the Cl−C covalent bond), and zero net effect in the equatorial directions. Modeling the anisotropy in

the charge distribution of the Cl atom with either ρ_2 or ρ_1 alone, we obtain a negative coefficient. However, with both parameters, ρ_2 takes a relatively large and negative value, while ρ_1 acts as a correction to give more detail to the shape and happens to take a small positive value. The shape of the Cl atomic charge density thus corresponds to the conventionally viewed cylindrical lone pair density. The anisotropic coefficients for the effective shape of the N and C atoms, as sampled by intermolecular contacts between cyanuric chloride molecules are even smaller in magnitude than ρ_1^{Cl}, and relatively insignificant. The anisotropy in the repulsion is consistent with the atomic multipolar representation of the molecular charge density. The DMA of the chlorine atoms shows a large quadrupole moment, significant dipole and negligible net charge, whereas the multipolar expansions of the charge distributions of the C and N atoms are dominated by large, nearly equal and opposite charges. Thus, the analytical anisotropic models derived by fitting the overlaps are consistent with the atomic charge distributions, as sampled in the intermolecular contact region.

2.1.2. Parametrization and Validation of the Repulsive Potential Using Intermolecular Perturbation Theory Calculations. The short-range repulsive intermolecular energy is dominated by the exchange-repulsion energy. However, the penetration energy, which is the modification of the electrostatic energy due to the overlap of the charge distributions, will also correlate with the overlap. The charge transfer between the molecules also decays exponentially, and so could be represented by a similar functional form. By using IMPT[3,28,29] calculations that compute these three components separately from the monomer wave function, we are able to assess whether one exponential repulsion model potential is able to effectively represent all these contributions, without significant loss in accuracy. Hence, the correlation of overlap with just the exchange-repulsion (ER), the exchange-repulsion plus penetration (ERP) and the exchange-repulsion plus penetration plus charge-transfer energies (ERPC) is tested by using these three different combinations of IMPT calculated energies as the repulsive potential energy surfaces E_{rep}.

The assumed relationship (eq 6) between the model atom−atom overlap and the corresponding contribution to the repulsion energy, and the anisotropic atom−atom model for the overlap (eq 8) gives

$$\begin{aligned} E_{rep}^{ik} &\cong K[S_{aniso}^{ik}]^y \\ &= K\sigma \exp([-y\alpha_{\iota\kappa}][R_{ik} - (\chi_0^{\iota\kappa} + \rho_1^{\iota}(\mathbf{z}_i\cdot\mathbf{R}_{ik}) + \\ &\quad \rho_1^{\kappa}(-\mathbf{z}_k\cdot\mathbf{R}_{ik}) + \rho_2^{\iota}(3[\mathbf{z}_i\cdot\mathbf{R}_{ik}]^2 - 1)/2 + \\ &\quad \rho_2^{\kappa}(3[\mathbf{z}_k\cdot\mathbf{R}_{ik}]^2 - 1)/2)]) \quad (10) \end{aligned}$$

The quantity $\sigma = s^y$ describes one unit of modified overlap. K describes the proportionality between the atom−atom contribution to the repulsion energy and the modified overlap between the atoms. We use the same value of K for all atom pairs. Comparing this with the model intermolecular potential (eq 1), gives $B_{\iota\kappa} = y\alpha_{\iota\kappa}$ and $A_{\iota\kappa} = K\sigma \exp(y\alpha_{\iota\kappa}\chi_0^{\iota\kappa})$, with the same parameters describing anisotropy in both the overlap and the repulsion. The power y is expected to be close to one. The model overlaps (S_{aniso}^{ik}, or for the isotropic model potential, S_{iso}^{ik}) are the same for all three definitions of E_{rep}, but the optimal values of y may differ between them. The K values are expected to decrease when the attractive penetration and charge-transfer energies are included in E_{rep}, although a comparison between K values is only really meaningful at constant y.

To obtain the constants (K) and powers (y) linking E_{rep} to the model overlap, we carry out Hayes-Stone IMPT[28] calculations at 20 of the randomly generated geometries. These geometries are chosen to ensure sampling so that 10 have total overlaps between 0.00005 and 0.0005 atomic units and the other 10 have overlaps between 0.0005 and 0.005 atomic units. This results in half the IMPT points having exchange-repulsion energies approximately between 1 and 10 kJ/mol and the rest sampling higher up the repulsive wall to about 100 kJ/mol.

The number of basis functions required for calculations on the cyanuric chloride dimer restricted the IMPT calculations to the 6-31G SCF level. For each geometry, the exchange-repulsion and charge-transfer[29] were calculated by IMPT, and the penetration energy as the difference between the electrostatic energy calculated by IMPT and from the DMA. This use of IMPT results calculated with a smaller basis set than the overlaps used in the fitting has proved a reasonable practical compromise in previous detailed studies.[17,18]

The K and y (if required) parameters were fitted for a variety of combinations of IMPT surface and overlap models, as shown in Table 3. The slight approximation in assuming that the

TABLE 3: Fits of Model Overlaps to Repulsive Potential Energy Surfaces[a]

terms in E_{rep}	K	y	rms % error	R
OM-iso Fully Isotropic; $E_{rep} = KS_{iso}$				
ER	9.710	*1*	19.5	0.9918
ERP	6.571	*1*	22.6	0.9931
ERPC	6.139	*1*	23.3	0.9933
OM-aniso Fully Anisotropic; $E_{rep} = KS_{aniso}$				
ER	8.357	*1*	17.2	0.9972
ERP	5.627	*1*	23.4	0.9911
ERPC	5.259	*1*	23.4	0.9917
OP-iso Fully Isotropic; $E_{rep} = KS_{iso}^y$				
ER	8.349	0.978	19.0	0.9920
ERP	5.654	*0.978*	21.2	0.9941
ERP	4.533	0.946	20.4	0.9952
ERPC	5.282	*0.978*	22.2	0.9942
ERPC	4.472	0.954	21.8	0.9950
OP-aniso Fully Anisotropic $E_{rep} = KS_{aniso}^y$				
ER	5.102	0.926	9.0	0.9992
ERP	3.444	*0.926*	13.2	0.9959
ERP	2.726	0.891	11.2	0.9974
ERPC	3.218	*0.926*	14.1	0.9963
ERPC	2.640	0.896	12.7	0.9974
Comparative Fits				
OP-anisoCl (Anisotropy on Cl Only; K Reoptimized To Minimize RMS % Error)				
ER	5.067	0.926	8.8	0.9996
ERP	2.703	0.891	11.4	0.9961
ERPC	2.618	0.896	12.9	0.9961
GM Proportionality to Actual Overlaps $E_{rep} = KS_{\rho}$				
ER	8.654	*1*	16.1	0.9987
ERP	5.826	*1*	22.1	0.9919
ERPC	5.444	*1*	22.1	0.9925
GP Proportionality to Actual Overlaps $E_{rep} = KS_{\rho}^y$				
ER	5.906	0.933	8.5	0.9993
ERP	3.283	0.899	10.3	0.9942
ERPC	3.133	0.903	11.5	0.9946

[a] The correlation coefficient, R, and the rms % error in fitting various relationships between the accurately calculated overlaps (S_ρ) and the isotropic (S_{iso}) and anisotropic (S_{aniso}) atom−atom models for the overlaps, to the IMPT calculated short-range repulsion energies. E_{rep} includes the exchange−repulsion (ER), plus penetration (ERP), plus charge-transfer (ERPC) energies. When the value of the power y is in italics, it has been assumed; otherwise, it was fitted along with K to minimize the RMS % error. The model labels distinguish modeled overlaps (O) from accurately calculated overlaps (G) and the assumption $y = 1$ (M) from the use of the power law (P).

TABLE 4: Transferable Potential Parameters for Aromatic C/N/Cl Compounds[a]

atoms ι and κ	$C_{\iota\kappa}$/kJ mol^{-1} Å^6	$B_{\iota\kappa}$/Å^{-1}	$A_{\iota\kappa}$/kJ mol^{-1}	$\rho^{\iota}_1 = \rho_{101}$/Å	$\rho^{\kappa}_1 = \rho_{011}$/Å	$\rho^{\iota}_2 = \rho_{202}$/Å	$\rho^{\kappa}_2 = \rho_{022}$/Å
Cl···Cl	5534.64	3.679257	1400327.6	0.02676	0.02676	−0.10115	−0.10115
N···N	1365.16	4.018114	920414.4	0	0	0	0
C···C	1539.89	4.055413	294160.2	0	0	0	0
Cl···N	2748.85	3.784438	949690.7	0.02676	0	−0.10115	0
Cl···C	2919.33	4.438507	3854905.2	0.02676	0	−0.10115	0
N···C	1419.96	3.907456	315074.2	0	0	0	0

[a] This potential of the form given by eq 1 was derived from the ERPC OP-anisotropic potential, retaining only the anisotropic coefficients on chlorine. When used in conjunction with an SCF DMA, it is denoted NE-aniso.

relationship for total repulsion energies and total overlaps (eq 6), can be also used for individual terms (eq 10), when y is slightly less than unity can be largely absorbed[16] into the optimization of K.

The test of the basic assumption of the overlap model is provided by the correlation of the IMPT repulsive energies with the total overlaps, as calculated directly by GMUL. The correlations are reasonable, particularly if the power model is used with $y \sim 0.9$. The rms error of approximately 10% in an exponential repulsive wall is inherent in making the overlap approximation and the errors in both the IMPT and overlap calculations with different basis sets.

In the context of this inherent error, the additional error produced by incorporating the penetration and charge-transfer energies into the same repulsion model is acceptable. Including the penetration energy along with the exchange-repulsion energy reduces the value of K, as would be expected from the inclusion of this attractive short range term, but only slightly decreases the accuracy of the fit, particularly if y is optimized. Inclusion of the charge-transfer term has a similar though smaller effect. Therefore the model repulsion can absorb these additional contributions to the intermolecular energy without significant loss in accuracy. In principle these additional energy terms would be expected to have a different approximate dependence on the overlap. Indeed, the penetration energy itself is actually best described by a power y that is slightly greater than 1. However, it is of opposite sign to the exchange-repulsion and in order best to express the combined term as a single function, a power less than 1 (and less than that of the exchange-repulsion alone) is optimal. However, the differences from using the same power of y as for the exchange repulsion alone are small, and so for convenience, the same y value is used in the repulsion potentials tested in the next section.

The quality of the fits of the atom−atom analytical models to the IMPT data in Table 3 show clearly that the combination of both anisotropy and the power law gives a very considerable improvement. These fits are substantially better than can be obtained in isolation from either modification to the basic overlap model.

It is also noticeable that the models with anisotropy only on chlorine and with anisotropy on all atoms are of essentially equal quality. This is consistent with the expectation that chlorine will be substantially more anisotropic than first row atoms[10] and consistent with the size of the anisotropic parameters in Table 1. However, this also reflects the accessibility of the chlorine to intermolecular contacts in cyanuric chloride. 99% of the total overlap in the test set of dimer geometries can be attributed to Cl···X pairs (49% Cl···N; 40% Cl···Cl; 10% Cl···C; 1% all other pairs), and so the sampling of the non-chlorine contacts is not significant because of the molecular geometry.

It is extremely encouraging that the best analytical model repulsion (OP-aniso) reproduces the IMPT repulsion surfaces almost as well as the accurately calculated overlaps (GP). Thus we believe that our OP-aniso model is almost as accurate as is possible for an overlap-based model of the repulsion energy.

3. Method of Testing of Model Potentials Using Experimental Crystal Structures

Several nonempirical potentials were tested for their ability to reproduce the *C*2/*c* crystal structure (VUGSIZ10) of cyanuric chloride, as determined by Pascal and Ho.[23,27] (This is very similar to the determination of Maginn et al.,[22] allowing for the different nonstandard setting of the same space group *I*2/*a*.) The intermolecular potentials tested (eq 1) incorporated the more successful repulsion models (as judged by the IMPT data, Table 3), based on the overlap raised to the power $y = 0.978$ for the isotropic and $y = 0.926$ for the anisotropic potentials. In addition, two slightly empirical models were derived, by fitting the K value to optimally reproduce the experimental cell volume. This was done to test whether experimental data could be used to derive K, so that the overlap model can be used without requiring IMPT data. This OP-VOL model, using the isotropic model overlaps with $y = 0.978$ gave $K = 4.406$, and using the anisotropic model for the overlap and $y = 0.926$ gave $K = 3.098$. These estimates of K are only slightly smaller than derived by fitting to the exchange-repulsion plus penetration and charge-transfer (ERPC) surfaces. This is consistent with the volume-optimized repulsion also absorbing small attractive contributions such as polarization, C_8 and C_{10} dispersion terms, and temperature effects.

For comparison, calculations were also carried out using an empirically fitted repulsion−dispersion potential with the same DMA electrostatic model. The Cl···Cl parameters had been fitted to the crystal structures and lattice energies of perchlorinated hydrocarbons by Hsu and Williams[15] and the carbon and nitrogen parameters had been fitted by the same group to azahydrocarbons.[39] The model potential constructed using these parameters and the combining rules for the heteroatomic interactions is denoted FIT. Although the parameters were derived in conjunction with an electrostatic model and appear to be the most appropriate available, this FIT potential has not previously been used with these functional groups, or with a DMA electrostatic model.

3.1. A Transferable Model Potential. The most theoretically complete nonempirical potential (the anisotropic potential OP-ERPC) was tested for its transferability to model the larger related molecules PIJBIT and PIJBOZ (Scheme 1). These molecules have an additional atomic type to cyanuric chloride, of an aromatic carbon that is not bonded to chlorine but to other carbon and nitrogen atoms. In the transferable scheme, all carbons had the same repulsion parameters and were treated as isotropic by removing the very small anisotropy coefficients ρ_1^{C} and ρ_2^{C}. Since the anisotropy on the N atoms was also relatively insignificant, ρ_1^{N} and the negligible ρ_2^{N}, were also left out. The final nonempirical potential parameters for this model NE-aniso, with anisotropy only on the Cl atoms, are given in Table 4.

TABLE 5: Reproductions of the Crystal Structure of Cyanuric Chloride (VUGSIZ10) by Lattice Energy Minimization[a]

model	expt	FIT	OP-ER	OP-ERP	OP-ERPC	OP-VOL	OP-ER	OP-ERP	OP-ERPC	OP-VOL
repulsion aniso			isotropic	isotropic	isotropic	isotropic	anisotropic	anisotropic	anisotropic	anisotropic
LE_{init}/kJ mol^{-1}		−74.29	−27.54	−51.14	−54.40	−62.09	−30.78	−53.49	−56.58	−61.83
LE/kJ mol^{-1}		−76.26	−45.51	−55.93	−58.07	−64.33	−43.74	−55.01	−57.35	−62.14
space group	*C*2/*c*	*R*$\bar{3}$*c*	*C*2/*c*	*C*2/*c*	*C*2/*c*	*C*2/*c*	*C*2/*c*	*C*2/*c*	*C*2/*c*	*C*2/*c*
a/Å	12.925	13.043	13.634	13.341	13.288	13.147	13.481	13.143	13.083	12.968
b/Å	7.455	7.524	7.857	7.686	7.655	7.573	7.776	7.581	7.547	7.481
c/Å	7.540	7.811	7.982	7.642	7.582	7.419	8.087	7.706	7.639	7.515
β/deg	120.1	123.9	121.0	121.4	121.5	121.6	119.8	120.2	120.3	120.4
$c \sin \beta$/Å	6.530	6.486	6.843	6.525	6.468	6.316	7.016	6.661	6.598	6.482
vol/Å^3	628.8	636.5	733.1	669.0	658.0	628.8	735.5	663.7	651.5	628.8
ρ/g cm^{-3}	1.948	1.925	1.671	1.831	1.862	1.948	1.666	1.846	1.880	1.948
N···Cl (1)	3.100	3.169	3.502	3.330	3.300	3.218	3.421	3.226	3.191	3.126
N···Cl (2,3)	3.112	3.167	3.515	3.347	3.317	3.236	3.428	3.235	3.200	3.234
angle (1)	180	180	180	180	180	180	180	180	180	180
angle (2,3)	173	180	174	174	174	173	174	174	174	174
rms % cell edges		2.2	5.6	2.7	2.3	1.6	5.5	1.9	1.3	0.3

[a] Lattice energies (LE) were calculated using a 15 Å cutoff on atom−atom distances for the repulsion and dispersion terms, Ewald summation for the charge−charge, charge-dipole, and dipole−dipole electrostatic terms, and a 15 Å cutoff on molecular centers for all the higher terms in the multipole expansion of the electrostatic energy up to R_{ik}^{-5}. The two inequivalent N···Cl intermolecular contacts are characterized by the N···Cl separation and the N···Cl−C angle. The rms % cell is the rms % error in the cell lengths.

This potential was used in conjunction with a DMA of the SCF 6-31G** wave function of the experimental molecular structure, as the molecules are too large to obtain a correlated wave function. The total quadrupole moment of cyanuric chloride is remarkably unchanged by the correlation of the wave function, and so the SCF multipoles were used unscaled, as there was no clear basis for deriving a scaling factor. However, the individual atomic charges are considerably larger, by around 50%, and so the neglect of the effect of electron correlation will certainly have produced more uncertainty into the electrostatic contribution to the lattice energy.

3.2. Methods of Modeling the Crystal Structures. The model potentials were tested for their ability to reproduce the experimental crystal structures by lattice energy minimization. The molecules were held rigid at their experimental molecular geometries. The program DMAREL,[40] was extended to use the anisotropic atom−atom repulsion model, and to minimize maintaining the space-group symmetry. The eigenvalues of the second derivative matrix, and the calculated elastic constants[41] were examined to ensure that true minima were found.

4. Results

4.1. Reproduction of Cyanuric Chloride Crystal Structure. Table 5 shows that the empirical FIT potential, while probably better than the isotropic potentials used by Magnin et al., still produces a minimum energy structure in which all the C−Cl···N contacts are linear. This produces flat layers and a higher symmetry *R*$\bar{3}$*c* structure, and the fish-scale effect is lost. In contrast, all the nonempirical potentials maintain the experimental fish-scale effect[22] (see Figure 1) and experimental symmetry, with the N···Cl−C angle being maintained around 173° for Cl2 and Cl3 and the intermolecular distance being slightly longer than in the linear N···Cl1 contact.

Although all the nonempirical potentials reproduce the fish-scale effect and the qualitative crystal structure, the minimum energy lattice parameters reduce and improve as the approximate inclusion of the penetration energy reduces the repulsion. The distance between the layers, as estimated by $c \sin \beta$ is then very reasonable for both the isotropic and anisotropic potentials. Further addition of the charge-transfer term makes a further improvement.

The anisotropic models all have better *a* and *b* lattice parameters than the isotropic equivalents, reflecting shorter N···Cl distances. The shape of the chlorine atom in cyanuric chloride exhibits polar flattening,[10] reflected by the sign of the anisotropic parameter ρ_2^{Cl}, giving chlorine its smallest van der Waals radius in the direction of the Cl···N contact. Thus the OP-aniso models improve the description of the *ab* plane, relative to the isotropic equivalents. The theoretically most accurate nonempirical model gives the best reproduction of the crystal structure, with an rms error of 1.3% in the cell lengths, and only overestimates both N···Cl distances by 0.09 Å.

The OP-VOL models, where the proportionality constant *K* was obtained by fitting to the cell volumes, confirms the improvement produced by including anisotropy in the repulsion. The anisotropic OP-VOL model reproduces the cell parameters with an 0.3% rms error, whereas the isotropic equivalent has to underestimate the interlayer spacing to improve the N···Cl contacts, giving an rms error of 1.6%.

The predicted lattice energies for cyanuric chloride become increasingly stable as the attractive short-range terms are included. Unfortunately, there is no experimental sublimation energy available. The regression analysis of Westwell et al.[42] based on the boiling points of a wide variety of substances, suggests a sublimation enthalpy of 56.5 kJ/mol for cyanuric chloride. A similar regression analysis, based on 12 chlorinated and other substituted aromatics and heteroaromatics similar to cyanuric chloride for which boiling points and sublimation enthalpies are available[43] predicts a sublimation enthalpy of 70.0 kJ/mol. Thus, the lattice energies predicted by the ERP, ERPC, and VOL potentials are reasonable, given the even larger errors implicit in using such correlations than in the usual comparison of lattice energies with heats of sublimation. We also note that there is a secondary minimum in the dimer potential energy surface that corresponds closely to the "in-plane" C−Cl···N interaction in the crystal. The energy is −5.7 kJ/mol for the nonempirical anisotropic OP-ERPC potential, in good agreement with the literature MP2 value of −5.1 kJ/mol[27] for a smaller model system for the Cl···N interaction. Thus the nonempirical potential is providing reasonable intermolecular energies.

4.2. Reproduction of Crystal Structures Using the Transferable Potential. The transferable potential model still reproduces the crystal structure of cyanuric chloride well (Table 6), including the fish scale effect with N···Cl2−C of 173°. The simplification of the potential by replacing the MP2 by an SCF DMA and removing the small anisotropic terms (Table 4) actually gives a slightly better reproduction of the crystal structure (contrast Table 6 with Table 5). The lattice energy is

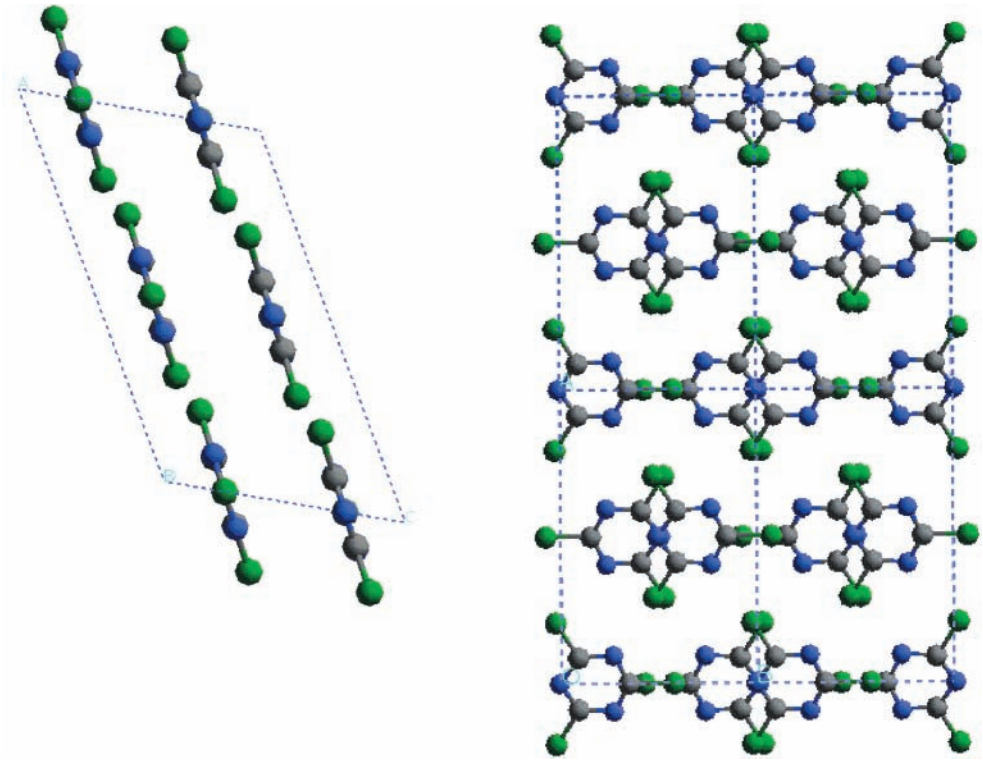

Figure 1. Crystal structure of cyanuric chloride:[27] (a) a view down the *b* axis showing the slight tilting of the molecules from the layer plane (the fish-scale effect); (b) a view down the *c* axis showing the superposition of the layers.

TABLE 6: Test of Transferable Potentials for Reproducing the Crystal Structures of Azaaromatic Chlorides[a]

	VUGSIZ			PIJBOZ			PIJBIT		
	expt[27]	FIT-iso	NE-aniso	expt[27]	FIT-iso	NE-aniso	expt[27]	FIT-iso	NE-aniso
a/Å	12.925	12.956	13.046	11.611	11.800	11.570	7.407	7.359	7.628
b/Å	7.455	7.518	7.558	5.923	5.785	5.950	7.714	7.508	7.541
c/Å	7.540	7.568	7.570	16.098	16.268	15.905	7.942	7.698	7.488
β/deg	120.1	121.3	119.8	122.7	124.4	121.4	97.12	95.98	93.23
rms % cell		0.55	0.99		1.75	0.77		2.38	3.94
ρ/g cm^{-3}	1.948	1.946	1.890	1.923	1.958	1.917	1.99	2.12	2.08
N···Cl/Å	3.100	3.163	3.203	3.284	3.271	3.308	3.207	2.997	3.035
N···Cl/Å	3.112	3.141	3.188	3.341	3.348	3.408	3.332	3.099	3.126
LE/kJ mol^{-1}		−79.9	−60.3		−117.1	−93.2		−167.2	−135.7

[a] Lattice energies (LE) were calculated using a 15 Å cutoff on atom−atom distances for the repulsion and dispersion terms, Ewald summation for the charge−charge, charge-dipole, and dipole−dipole electrostatic terms, and a 15 Å cutoff on molecular centers for all the higher terms in the multipole expansion of the electrostatic energy up to R_{ik}^{-5}. The rms % cell is the rms % error in the cell lengths.

somewhat greater with the electrostatic model derived from the less realistic wave function. This change in the electrostatic model qualitatively improves the crystal structure reproduction by the FIT potential, as the correct space group is maintained. The cell parameters and Cl···N interactions are significantly improved and the C−Cl(2,3)···N angles becomes 173°, preserving the fish-scale effect. The differences between the crystal cell length reproductions using the two electrostatic models are not significant compared with errors in comparing lattice energy minima with room-temperature crystal structures.[44]

The crystal structure reproduction of PIJBOZ, the compound whose asymmetry precludes a layer structure, is very reasonable for both the empirical isotropic and nonempirical anisotropic model potential, both being well within the errors of static lattice energy minimization. Both the N···Cl contact distances and the cell parameters are well reproduced. The second layer structure, PIJBIT was less satisfactorily reproduced by either potential, as both underestimated the longer N···Cl contacts. The overall cell volume contraction of 6% for FIT represents a reasonable contraction in all lattice parameters. The corresponding volume contraction of 4.5% for the nonempirical potential represents a larger distortion of the *ac* plane. There was a significant slippage of the layers in PIJBIT, with the most marked change in an intermolecular contact being a shortening of the closest Cl···C3 distance from 3.545 to 3.321 Å. For the empirical FIT potential, this distance only shortened by 0.13 Å to double its contribution to the repulsion. Since this involves a junction C atom, it appears that the problem with the NE-aniso potential arises from assuming that the junction C atoms have a similar repulsion to C atoms bonded to Cl and two N atoms.

5. Discussion

Cyanuric chloride molecules interact through Cl···Cl and N···Cl contacts, whose nature has been the subject of considerable debate.[12,13] We have developed nonempirical potentials for cyanuric chloride, which include both anisotropy in the repulsive wall of the Cl and N atoms and the penetration and charge-transfer energies. The comparison of these potentials with the IMPT potential surface and also the reproduction of the crystal

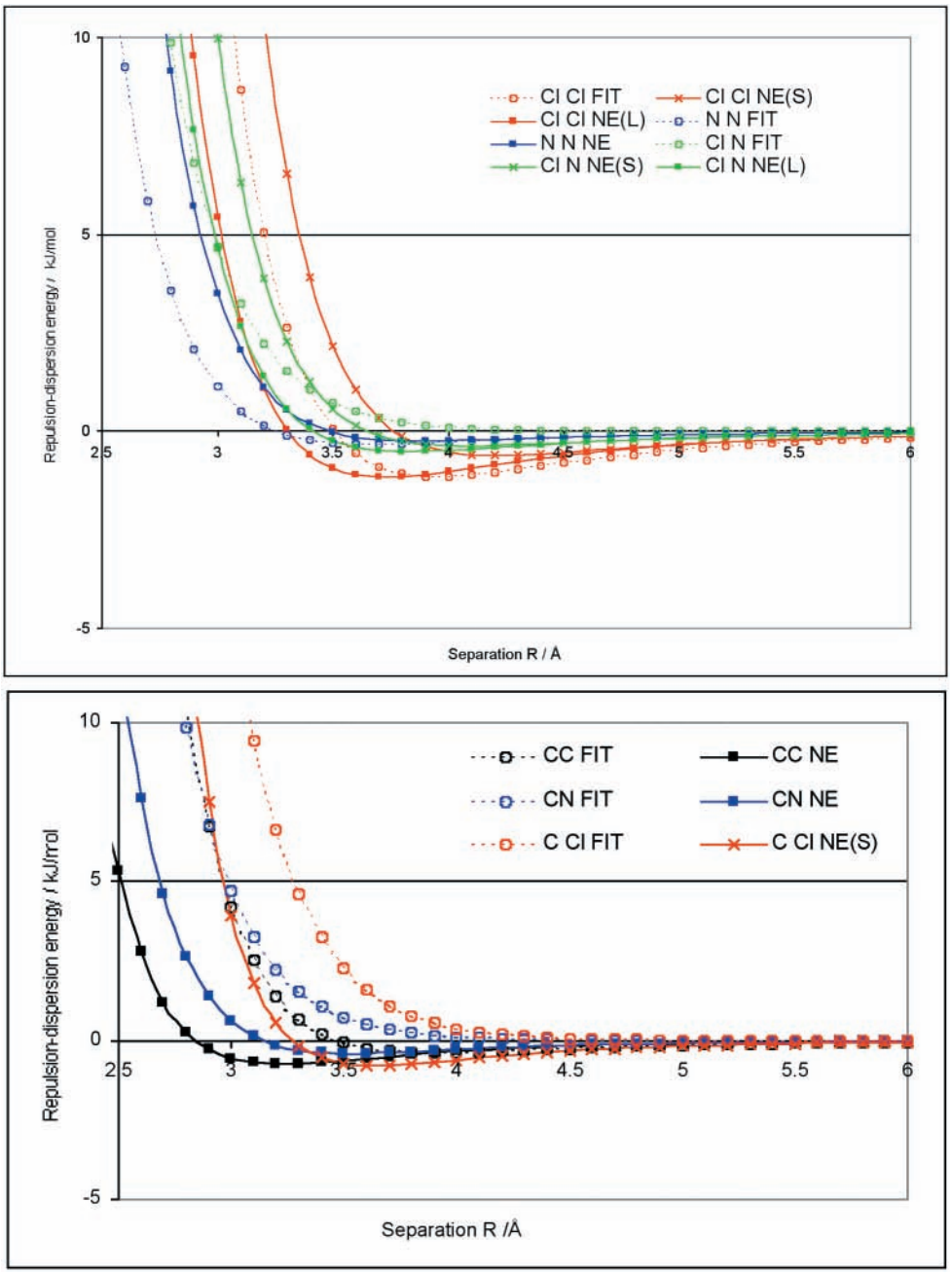

Figure 2. Comparison of the repulsion−dispersion potentials derived using the transferable nonempirical potential with anisotropy on the Cl atoms (NE-aniso) with the empirical potential FIT. (a) The anisotropy of the Cl interactions is demonstrated by contrasting the linear ($\mathbf{z}_1\cdot\mathbf{R} = -\mathbf{z}_2\cdot\mathbf{R} = 1$) arrangement L with the side-on conformation S ($\mathbf{z}_1\cdot\mathbf{R} = -\mathbf{z}_2\cdot\mathbf{R} = 0$). (b) The smaller repulsion of carbon atoms in the nonempirical potential for cyanuric chloride is demonstrated for the side-on (S) interactions with carbon.

structures, are in accord with the conclusions of detailed studies of these specific contacts from crystal structure analysis and IMPT calculations on smaller model systems.[12,13] We find that the anisotropy of the atom−atom overlaps involving Cl atoms is significant, producing a marked polar flattening of the repulsive wall around Cl atoms (Figure 2a). The charge-transfer is not negligible, but the electrostatic and dispersion terms contribute more to the attractive nature of these contacts. This is fortunate, as if the transfer of charge in this "donor−acceptor" interaction were significant, the intermolecular potential could not be approximated as pairwise additive, as required by current modeling programs.

Thus, this study has shown that the overlap model can be used in order to parametrize anisotropic repulsion potentials for organic molecules. The calculation of the overlap at a wide range of geometries of the molecules in the intermolecular repulsive region ensures that the atom−atom overlaps sample the orientation dependence of possible intermolecular contacts. The fitting of each atom−atom overlap allows the functional form of the anisotropy to be determined and parametrized, if it is significant. However, only atoms with very nonspherical charge distributions with a large accessible surface are likely to require anisotropic repulsion potentials. In this case, the chlorine atoms are shown by the analysis of the overlaps to have significant anisotropic repulsion (Figure 2a), which is consistent with all the experimental evidence for the polar flattening of their effective van der Waals radii. The introduction of the simple anisotropic atom−atom functional form (eq 8) allows the overlap between the charge densities to be modeled analytically very successfully (Table 2).

Having modeled the overlap between the molecules, then using this to produce a model repulsion potential depends on the realism of the assumed relationship. The comparison with IMPT estimates of the repulsive energies shows that this is a reasonable practical assumption for cyanuric chloride, similar to that found for other organic systems such as amides[16] and oxalic acid.[17] The basic relationship, $E_{rep} = K[S_\rho]^y$, necessarily limits the accuracy of the repulsion model. This accuracy is not seriously compromised by using the same functional form to include the penetration and charge-transfer energies in the repulsion model, as found for the amides.

Although this analysis against IMPT data is vital in developing the overlap model, it becomes impractical for larger organic molecules. Indeed, the whole point of the overlap model is as a means of estimating the repulsion potential for molecules where it is impractical to calculate sufficient points of sufficient quality on an ab initio potential energy surface to allow a well defined fitting of the model potential. Even for cyanuric chloride, the computational demands of calculating sufficient points on a moderate quality IMPT surface for validation were large. However, if the relationship between the repulsion potential and the readily modeled overlap is assumed (including a value of y), then other methods could be used to estimate the proportionality parameter K. The fitting of this one parameter to the volume of the crystal structure (OP-VOL) provides an illustration of this approach.

The more practical validation of the overlap derived repulsion potentials comes from their use in modeling the crystal structures, in conjunction with an atomic multipolar electrostatic and atom−atom dispersion model. The nonempirical potentials with the best repulsion models (as judged on theoretical grounds and against the IMPT data) reproduce the crystal structures competitively with the best empirically derived repulsion−dispersion potentials, which had been fitted to reproduce crystal structures.

Once the penetration and charge-transfer terms are incorporated, all the nonempirical potentials reproduce the lattice parameters of cyanuric chloride within the few percent error that may be attributable to the errors in comparing static lattice energy minima with room-temperature crystal structures.[44] The inclusion of anisotropy improves the N···Cl close contact distances.

All the nonempirical potentials are able to reproduce the fish-scale effect and hence space group of the cyanuric chloride crystal structure. This effect was attributed by Ho et al.[27] to relieving the intralayer steric interactions between Cl atoms. The reasonable proposal by Magnin et al.,[22] that the fish scale effect was caused by anisotropy in the Cl···N interactions, seems unlikely from our results. It cannot arise from repulsion anisotropy, as the fish scale effect is reproduced by our isotropic repulsion potentials. The anisotropy in the atom−atom electrostatic interactions is included with the empirical FIT potential, and this minimizes to the higher symmetry structure with an MP2 quality electrostatic model. The small differences between the D_{3h} gas phase and the crystallographic C_{2v} symmetry of the molecule are unlikely to cause the effect, as we found that using the ab initio optimized D_{3h} monomer instead of the experimental structure had very little effect on the crystal structure minimizations.

It seems likely that the fish-scale effect may be produced by the balance of the different atom−atom interactions between the layers. The empirical FIT potential only reproduced this effect when the c cell parameter, which determines the interlayer distance, was very well reproduced with the stronger electrostatic interactions. The dimer structure is predicted to be an offset stacked structure, mainly stabilized by the dispersion energy, with a much smaller interplanar angle of 11° for the anisotropic OP-ERPC potential than the 60° predicted by the FIT potential. This is consistent with semiempirical calculations on one layer of nine cyanuric chloride molecules not showing the fish scale effect.[22]

The results of modeling two larger azaaromatic chloride crystal structures with the same empirical potential and a nonempirical potential derived from OP-ERPC also suggest sensitivity to stacking interactions. The Cl···N contacts are well modeled in both structures. However, the layer structure of PIJBIT is less well reproduced, with an even larger slippage between the stacked layers in the nonempirical potential than in the empirical potential. A cause for this appears to be an underestimate of the repulsion arising from the bridging C atom. The graph (Figure 2b) contrasting the empirical and nonempirical repulsion−dispersion interactions with carbon clearly shows that the overlap model is predicting a smaller repulsive wall for carbon. It seems plausible that this smaller repulsion, which will only affect the interlayer contacts, favors the fish-scale effect in cyanuric chloride but is inappropriate for the bridging C atom in PIJBIT. It is reasonable that a carbon bonded to a chlorine and two nitrogen atoms should have less associated electron density, and thus have its repulsive wall extend less far above the aromatic ring than in an aromatic hydrocarbon. Thus, this study, like that of oxalic acid,[17] shows the applicability of the overlap model for deriving specific intermolecular potentials for molecules where assuming transferability is a poor approximation.

Thus, the overlap model allows the development of nonempirical repulsion potentials that reflect the atomic charge distributions within specific molecules, including their anisotropy. The model could be further improved for specific molecules by increasing the accuracy of the benchmark calculations of the ab initio repulsive potential energy surface, for example, by using an estimate of the repulsion terms from a correlated wave function using symmetry adapted perturbation theory.[45] It may also be worthwhile increasing the accuracy with which the overlaps are calculated by using a larger basis set.[17] However, the accuracy will always be limited by the assumption of the functional relationship between overlap and the short-range energy terms. Similarly, the accuracy of the total nonempirical potential will also be limited by the modeling of the other contributions. The electrostatic term is well modeled by the DMA, with the effect of the onset of overlap of the charge distributions accounted for by incorporating the penetration energy into the repulsion model. However, the dispersion potential is crudely modeled, and our model excludes the polarization energy. Nevertheless, the overlap model, by providing a basis for splitting the repulsive potential into atom−atom contributions and testing their anisotropy will help the development of more accurate nonempirical potentials for organic molecules following the improvement in potentials for small polyatomics.[3]

The success of the OP-VOL potential for cyanuric chloride and the transferable potential for PIJBOZ do show that the overlap model can be used to develop intermolecular potentials for molecules that are too large for the calculation of even a small number of IMPT points. PIJBIT, however, does show that the transferability of atomic types has to be considered carefully. Nevertheless, the success of these potentials with a far smaller number of empirical assumptions than are usually used for organic crystal structure modeling, does show that worthwhile

model potentials can be obtained essentially from the wave function of the isolated molecule.

6. Conclusions

To better model Cl···Cl and N···Cl interactions, we have developed a model anisotropic atom−atom intermolecular potential for cyanuric chloride, which incorporates both the anisotropy of the repulsive wall around the chlorine atom and the penetration and charge-transfer energies. This model successfully accounts for the crystal structures of cyanuric chloride and closely related azaaromatic chlorides.

Thus, this study has demonstrated that considering the overlap of the molecular charge distributions provides a practical method of determining whether the repulsive wall around an atom is anisotropic, and parametrizing that anisotropy. It also allows atom−atom repulsion potentials for small organic molecules to be parametrized without transferability assumptions. Although using the overlap model inevitably introduces some approximations, the approach has generated completely nonempirical model potentials that reproduce crystal structures at least competitively with potentials that were fitted to crystal structures. Thus, this approach shows considerable promise for deriving atom−atom potential parameters for organic functional groups where empirical parametrization is inadequate or impossible.

Acknowledgment. Helen Tsui (UCL) and Julian Cherryman (Avecia) for useful discussions, and Graeme Day (UCL) for assistance with the development of DMAREL to use anisotropic repulsion. This work was funded by Avecia and AstraZeneca through the Zeneca Strategic Research Fund.

References and Notes

(1) Stone, A. J.; Price, S. L. *J. Phys. Chem.* **1988**, *92*, 3325.
(2) Price, S. L. In *Reviews in Computational Chemistry*; Lipkopwitz, K. B., Boyd, D. B., Eds., 2000; Vol. 14, p 225.
(3) Stone, A. J. *The Theory of Intermolecular Forces*; Clarendon Press: Oxford, U.K., 1996.
(4) Buckingham, A. D.; Fowler, P. W.; Stone, A. J. *Int. Rev. Phys. Chem.* **1986**, *5*, 107.
(5) Coombes, D. S.; Price, S. L.; Willock, D. J.; Leslie, M. *J. Phys. Chem.* **1996**, *100*, 7352.
(6) Price, S. L. *Mol. Phys.* **1986**, *58*, 651.
(7) Brobjer, J. T.; Murrell, J. N. *Mol. Phys.* **1983**, *50*, 855.
(8) Peebles, S. A.; Fowler, P. W.; Legon, A. C. *Chem. Phys. Lett.* **1995**, *240*, 130.
(9) Wheatley, R. J.; Price, S. L. *Mol. Phys.* **1990**, *71*, 1381.
(10) Nyburg, S. C.; Faerman, C. H. *Acta Crystallogr. B* **1985**, *41*, 274.
(11) Desiraju, G. R.; Parthasarathy, R. *J. Am. Chem. Soc.* **1989**, *111*, 8725.
(12) Price, S. L.; Stone, A. J.; Lucas, J.; Rowland, R. S.; Thornley, A. E. *J. Am. Chem. Soc.* **1994**, *116*, 4910.
(13) Lommerse, J. P. M.; Stone, A. J.; Taylor, R.; Allen, F. H. *J. Am. Chem. Soc.* **1996**, *118*, 3108.
(14) Price, S. L.; Stone, A. J. *Mol. Phys.* **1982**, *47*, 1457.
(15) Hsu, L.-Y.; Williams, D. E. *Acta Crystallogr.* **1980**, *A36*, 277.
(16) Mitchell, J. B. O.; Price, S. L. *J. Phys. Chem. A* **2000**, *104*, 10958.
(17) Nobeli, I.; Price, S. L. *J. Phys. Chem. A* **1999**, *103*, 6448.
(18) Tsui, H. H. Y.; Price, S. L. *CrystEngComm* **1999**, *7*.
(19) Nobeli, I.; Price, S. L.; Wheatley, R. J. *Mol. Phys.* **1998**, *95*, 525.
(20) Wheatley, R. J.; Mitchell, J. B. O. *J. Comput. Chem.* **1994**, *15*, 1187.
(21) Wheatley, R. J. GMUL 3s. An extension to the GMUL program (version 3) that calculates an analytical form for the overlap of distributed charge densities. University of Nottingham, 1997.
(22) Maginn, S. J.; Compton, R. G.; Harding, M. S.; Brennan, C. M.; Docherty, R. *Tetrahedron Lett.* **1993**, *34*, 4349.
(23) Pascal, R. A.; Ho, D. M. *Tetrahedron Lett.* **1992**, *33*, 4707.
(24) CERIUS, 3.0.2 ed.; Molecular Simulations Inc.: Cambridge, U.K., 1992.
(25) Groger, H.; Sans, J.; Guthner, T. *Chimia Oggi* **2000**, *18*, 12.
(26) Lommerse, J. P. M.; Motherwell, W. D. S.; Ammon, H. L.; Dunitz, J. D.; Gavezzotti, A.; Hofmann, D. W. M.; Leusen, F. J. J.; Mooij, W. T. M.; Price, S. L.; Schweizer, B.; Schmidt, M. U.; van Eijck, B. P.; Verwer, P.; Williams, D. E. *Acta Crystallogr. B* **2000**, *56*, 697.
(27) Xu, K.; Ho, D. M.; Pascal, R. A. *J. Am. Chem. Soc.* **1994**, *116*, 105.
(28) Hayes, I. C.; Stone, A. J. *Mol. Phys.* **1984**, *53*, 83.
(29) Stone, A. J. *Chem. Phys. Lett.* **1993**, *211*, 101.
(30) Ioannou, A. G. Ph.D. Thesis, University of Cambridge, 1998.
(31) Halgren, T. A. *J. Am. Chem. Soc.* **1992**, *114*, 7827.
(32) Stone, A. J.; Alderton, M. *Mol. Phys.* **1985**, *56*, 1047.
(33) Price, S. L.; Stone, A. J.; Alderton, M. *Mol. Phys.* **1984**, *52*, 987.
(34) Wheatley, R. J.; Price, S. L. *Mol. Phys.* **1990**, *69*, 507.
(35) Price, S. L. *Mol. Phys.* **1987**, *62*, 45.
(36) Pai, S. V.; Chabalowski, C. F.; Rice, B. M. *J. Phys. Chem. A* **1997**, *101*, 3400.
(37) R. D. Amos, with contributions from I. L. Alberts, J. S. Andrews, S. M. Colwell, N. C. Handy, D. Jayatilaka, P. J. Knowles, R. Kobayashi, N. Koga, K. E. Laidig, G. Laming, A. Lee, P. E. Maslen, C. W. Murray, J. E. Rice, E. D. Simandiras, A. J. Stone, M. D. Su and DJ Tozer. CADPAC6: The Cambridge Analytical Derivatives Package; 6.0 ed. Cambridge, 1995.
(38) Wheatley, R. J. *Mol. Phys.* **1993**, *79*, 597.
(39) Williams, D. E.; Cox, S. R. *Acta Crystallogr. B* **1984**, *40*, 404.
(40) Willock, D. J.; Price, S. L.; Leslie, M.; Catlow, C. R. A. *J. Comput. Chem.* **1995**, *16*, 628.
(41) Day, G. M.; Price, S. L.; Leslie, M. *Cryst. Growth Des.* **2001**, *1*, 13.
(42) Westwell, M. S.; Searle, M. S.; Wales, D. J.; Williams, D. H. *J. Am. Chem. Soc.* **1995**, *117*, 5013.
(43) Chickos, J. S. Heat of Sublimation Data. In *NIST Chemistry WebBook;* NIST Standard Reference Database; Mallard, W. G., Linstrom, P. J., Eds.; National Institute of Standards and Technology: Gaithersburg, MD 20899, 1998; http://webbook.nist.gov, Vol. 69.
(44) Beyer, T.; Price, S. L. *CrystEngComm* **2000**, *34*, 1.
(45) Jeziorski, B.; Moszynski, R.; Szalewicz, K. *Chem. Rev.* **1994**, *94*, 1887.